Extended Abstracts of the 18th (1986 International) Conference on Solid State Devices and Materials, Tokyo, 1986, pp. 335-338

Negative Differential Mobility and Drift Velocity Overshoot in Single Quantum Well of AlGaAs/GaAs/AlGaAs Heterostructure

K. Miyatsuji, H. Tanimoto and C. Hamaguchi

Department of Electronics, Faculty of Engineering, Osaka University

Suita City, Osaka, 565 Japan

Monte Carlo simulation of hot electron transport in a quantum well AlGaAs/GaAs/AlGaAs is made to clarify the drift velocity overshoot and steady state drift velocity versus electric field relation. Conduction band discontinuities at the L- and X-points are estimated from the energy band calculation. Electronic subbands are calculated self-consistently and used for the simulation. Results are given for GaAs-well width of 500A and electron sheet density of $1\times10^{12}cm^{-2}$ at 77K. Drift velocity overshoot of $10^{8}cm/s$ appears at about 0.7ps at 10kV/cm. The maximum steady state drift velocity is $2.6\times10^{7}cm/s$ and negative differential mobility appears.

§1. Introduction

Heterojunction devices have received a considerable attention because of their high speed operation and various applications. However, their high field characteristics are known only a little from the point of both experimental and theoretical aspects. This is mainly due to the facts that electrons populate several subbands, resulting in a complicated situation to analyze the transport properties and that treatment of the scattering processes of the two-dimensional (2D) electrons is not well established. Inoue pointed out that high field transport properties of two-dimensional electrons are affected strongly by the subband structure of the quantized electrons.[1] Sasa et al. estimated the mobilities of electrons in an asymmetric single quantum well from Hall effect and Shubnikov-de Haas measurements, and found that the mobility of the electrons localized at the normal interface is larger than that at the inverted interface reflecting an importance of the impurity scattering for low field mobility.[2] Very simplified Monte Carlo simulations have been reported,[3,4] where the electrons with the energy exceeding the AlGaAs barrier and the electrons in the L-valleys are three dimensional in HEMT structure. Monte Carlo simulations of 2D electrons in Si inversion layers have been reported by Terashima et al.[5]

In this paper we report for the first time that the electrons transferred into the L-valleys are two-dimensional and that the electron transfer from the Γ-valley subbands to the L-valley subbands results in differential negative mobility. In addition the overshoot is very large, reaching about $10^{8}cm/s$ at 0.7ps at 10kV/cm and at 77K.

§2. Energy Band Diagram

Energy band structures of GaAs and AlGaAs can be calculated by using the empirical pseudopotential method or $\vec{k}\cdot\vec{p}$ perturbation method.[6,7] In the present work we used the pseudopotential method and obtained the energy gaps E_g=1.415eV, $E_{\Gamma L}$=0.31eV, and $E_{\Gamma X}$=0.38eV for GaAs and E_g=2.0eV, $E_{\Gamma L}$=0.30eV, and $E_{\Gamma X}$=0.14eV for $Al_xGa_{1-x}As$ (x=0.3). When we assume the conduction band discontinuity 0.3eV at the Γ-point we obtain the conduction band discontinuity ΔE_L=0.29eV and ΔE_X=0.06eV. On the other hand experimental results[8] indicate the band discontinuity ΔE_L=0.1eV and ΔE_X=-0.05eV for ΔE_Γ=0.3eV. Because of the ambiguity of the calculations and experimental data we choose ΔE_Γ=0.3eV, ΔE_L=0.2eV and ΔE_X=0.15eV. The following calculations are not influenced so much even if we choose different values. It should be pointed out that the scattering probabilities between 2D electron states and 3D electron states cannot be calculated because of the lack of the knowledge of the third k-vector, k_z, which is unknown for the electrons quantized in the z-direction. In addition

quantization of the electrons appears only when the conduction band discontinuity $\Delta E>0.1$eV for 500A well. Therefore in the present work we choose $\Delta E_X=0.15$eV.

We calculated the electronic subbands in Γ-, L- and X-valleys using the method reported elsewhere.[9,10,11] Assuming that all the electrons populate in the Γ-valley subbands, we obtained the subband energies, wave functions and the population of the electrons. These calculations determine the energy band bending at the Γ-point and thus at the L- and X-points.

§3. Scattering Probabilities of 2D Electrons

We proceed calculations of the scattering probabilities of 2D electrons using the results of Price.[12] The wave function and energy of 2D electrons in n-th subband in valley i are given by

$$\Psi_i = F_{in}(z)\exp(i\vec{k}\cdot\vec{r}) \tag{1}$$

$$E_{in}(\vec{k}) = \frac{\hbar^2k^2}{2m_i^*} + E_{in} \tag{2}$$

where $\vec{k}$ and $\vec{r}$ are the wavevector in the plane perpendicular to the z direction, and $F_{in}(z)$ and E_{in} are given by solving

$$[-\frac{\hbar^2}{2m_i^*}\frac{d^2}{dz^2}+ V(z)]\ F_{in}(z) = E_{in}F_{in}(z). \tag{3}$$

Transition probability of an electron with phonon emission or absorption from a state $\vec{k}_1$ and energy $E_{im}(\vec{k}_1)$ in the subband m to a state $\vec{k}_2$ and $E_{in}(\vec{k}_2)$ in the subband n is given by

$$W^{\pm}_{i,m\to n}(\vec{k}_1,\vec{k}_2) = \frac{2\pi}{\hbar}|M^{\pm}_{i,mn}(\vec{q})|^2\ \delta(E_{in}(\vec{k}_2) - E_{im}(\vec{k}_1) \pm \hbar\omega_q) \tag{4}$$

where the matrix element $M^{\pm}_{i,mn}(\vec{q})$ is

$$M^{\pm}_{i,mn}(\vec{q}) = (\frac{n_q+\frac{1}{2}\pm\frac{1}{2}}{V})^{\frac{1}{2}}\delta_{\vec{k}_1,\vec{k}_2\pm\vec{Q}}\ J^{\pm}_{i,mn}(q_z)\ C_q. \tag{5}$$

Here phonon wave vector is $\vec{q} = (\vec{Q},q_z)$ and n_q is the phonon occupation number and

$$n_q = 1/[\exp(\hbar\omega_q/k_BT)-1] \tag{6}$$

$$J^{\pm}_{i,mn}(q_z) = \int F_{im}(z)F_{in}(z)\exp(\pm iq_zz)dz. \tag{7}$$

In the case of acoustic phonon deformation potential scattering we have

$$C_q^{\,2} = \hbar D^2q^2/2\rho\omega_q \tag{8}$$

where D is the deformation potential and ρ is the density of the material. After some calculations we obtain

$$W_{i,m\to n}(\vec{k}_1) = W^{+}_{i,m\to n}(\vec{k}_1) + W^{-}_{i,m\to n}(\vec{k}_1)$$
$$= \frac{D^2k_BTm_i^*}{\pi\hbar^3\rho S_1^{\,2}}\int|F_{im}(z)|^2\ |F_{in}(z)|^2\ dz$$
$$\times\ u[E_{im}(\vec{k}_1)-E_{in}] \tag{9}$$

where S_1 is sound velocity and $u[E_{im}(\vec{k}_1)-E_{in}]$ is the step function, indicating that the inter-subband scattering occurs only when the total energy of the electron $E_{im}(\vec{k}_1)$ exceeds the subband energy E_{in}.

For polar optical phonon scattering

$$C_q^{\,2} = \frac{e^2\hbar\omega_{LO}}{2\varepsilon_oq^2}\left(\frac{1}{\kappa_\infty} - \frac{1}{\kappa_o}\right) \tag{10}$$

where $\kappa_o\varepsilon_o$ and $\kappa_\infty\varepsilon_o$ are the static and optical dielectric constants and finally we obtain

$$W_{i,m\to n}(\vec{k}_1) = \begin{cases} 0\ ;\ D<0 \\ \dfrac{e^2\omega_{LO}m_i^*}{8\pi\hbar^2\varepsilon_o}\left(\dfrac{1}{\kappa_\infty}-\dfrac{1}{\kappa_o}\right)\left(n_q+\dfrac{1}{2}\pm\dfrac{1}{2}\right) \\ \times\ \displaystyle\int_0^{2\pi}\frac{H_{i,mn}(Q)}{Q}d\theta\ ;\ D\geq 0 \end{cases}. \tag{11}$$

Here $H_{i,mn}(Q)$ is given by

$$H_{i,mn}(Q) = \int F_{im}(z_1)F_{in}(z_1)F_{im}(z_2)F_{in}(z_2)$$
$$\times\ \exp[-Q|z_1-z_2|]\ dz_1dz_2 \tag{12}$$

$$D = k_1^{\,2} - (2m_i^*/\hbar^2)(E_{in} - E_{im} \pm \hbar\omega_{LO}) \tag{13}$$

and

$$Q(\theta) = (k_1^{\,2} + D - 2k_1\sqrt{D}\cos\theta)^{\frac{1}{2}}. \tag{14}$$

For intervalley phonon scattering we have

$$C_q^{\,2} = \hbar D_{ij}^{\,2}/2\omega_{ij}\rho \tag{15}$$

and therefore the scattering probability is given by

$$W^{\pm}_{i\to j,m\to n}(\vec{k}_1) = \frac{n_v D^2_{ij} m_j^*}{2\hbar^2 \rho \omega_{ij}} \left(n_{ij} + \frac{1}{2} \pm \frac{1}{2}\right) \int |F_{im}(z)|^2 |F_{jn}(z)|^2 dz \times u[E_{im}(\vec{k}_1) - E_{jn} - \Delta_{ij} \mp \hbar\omega_{ij}] \quad (16)$$

where n_v is the number of equivalent valleys, $\hbar\omega_{ij}$ the intervalley phonon energy, Δ_{ij} the energy separation of the different valleys and E_{jn} is the n-th subband energy in the valley j.

At low electric fields impurity scattering is very important. Here we used the results of Price for the impurity scattering screened by 2D electrons.[13] The result is given by

$$W_{i,mn}(\vec{k}_1) = \begin{cases} 0 \; ; \; D = k_1^2 - (2m_i^*/\hbar^2)(E_{in} - E_{im}) < 0 \\ \dfrac{e^4 m_i^*}{8\pi\hbar^3(\kappa\varepsilon_o)^2} \displaystyle\int_0^{2\pi} \frac{I_{i,mn}(Q)}{[Q + PH_{i,mn}(Q)]^2} d\theta \\ \quad ; \; D \geq 0 \end{cases} \quad (17)$$

where

$$I_{i,mn}(Q) = \int N_d(z_o) \left[\int F_{im}(z) F_{in}(z) \exp(-Q|z - z_o|) dz\right]^2 dz_o . \quad (18)$$

$N_d(z_o)$ is donor distribution and

$$P = e^2 N_s / \kappa\varepsilon_o k_B T. \quad (19)$$

4. Monte Carlo Simulation of 2D Electrons in a Single Quantum Well

Using the results of the self-consistent calculations we obtained the scattering probabilities in a single quantum well $Al_xGa_{1-x}As/GaAs/Al_xGa_{1-x}As$ (x=0.3, GaAs-well width 500A). The parameters used in the present simulations are those reported by Littlejohn et al.[14] because electrons are mainly confined in the GaAs-well and thus their transport is determined by the parameters in GaAs. Energy band parameters are given in §2. Donors of 1×10^{18} cm^{-3} are assumed to distribute uniformly in the barrier regions of AlGaAs, one side with a spacer region of 60A and the other side without a spacer region. We considered the four lowest electronic subbands at each valley. Figure 1 represents the calculated drift velocity as a function of the electric field at 77K, where we find that the maximum drift velocity is about 2.6×10^7 cm/s at 2 kV/cm and negative differential mobility appears beyond this field. It is very interesting that the ohmic mobility is quite high and reaches 8×10^4 cm^2/Vs at 77K which is very close to the value we measured in a sample with the same structure described here. This means that the parameters of the Γ-valley used in the present work are precise. In Fig. 2 we present the occupation of the electrons in the three valleys. Here we find that electrons in the Γ-valley subbands decrease with increasing the electric field and the electron population in the L-valley subbands increases at electric field beyond 2kV/cm. The population in the X-valley is not appreciable and thus we can neglect intervalley transfer to the X-valleys in a simplified case. This indicates also that the energy band ordering at the X-point is not so important in AlGaAs/GaAs heterostructures. The occupation of the electrons in the subbands in Γ- and L-valleys is shown in Fig. 3. At electric fields below 2kV/cm repopulation of electrons occur within the subbands in the Γ-valley.

Figure 4 represents time evolution of the drift velocity in uniform electric field 1, 5 and 10 kV/cm at 77K, where the average drift velocity is shown. The maximum overshoot 10×10^7cm/s appears at about 0.7ps. In order to clarify the valley transfer of the electrons we plotted the drift velocities as a function of time in Γ-, L- and X-valleys in Fig. 5 at 10kV/cm. We find in Fig. 5 that the maximum drift velocity in the Γ-valley is about 14×10^7 cm/s which is much larger than the maximum value reported in bulk GaAs. Such a high value seems to reflect that the scattering probabilities of 2D electrons are quite different from those of 3D electrons.

In Fig. 6 occupation of the electrons in the three valleys is plotted as a function of time for the case of 10kV/cm. Note that increase in the upper valley population corresponds to the point where the drift velocity maximum occurs.

References
1) M. Inoue, S. Hiyamizu, M. Inayama and Y. Inuishi, Jpn. J. Appl. Phys. 22 Suppl. 22-1 (1983) 357.
2) S. Sasa, J. Saito, K. Nanbu, T. Ishikawa, S. Hiyamizu and M. Inoue, Jpn. J. Appl. Phys. 24 (1985) L281.
3) M. Tomizawa, K. Yokoyama and A. Yoshii, IEEE Electron Device Lett. EDL-5 (1984) 464.
4) K. Yokoyama and K. Hess, MSS-II Kyoto (1985) 533.
5) K. Terashima, C. Hamaguchi and K. Taniguchi, Superlattices and Microstructures, 1 (1985) 15.
6) M. L. Cohen and T. K. Bergstresser, Phys. Rev. 141 (1966) 789.
7) F. H. Pollak, C. W. Higginbotham and M. Cardona, J. Phys. Soc. Jpn. 21 Suppl.(1966) 20.
8) H. J. Lee, L. Y. Juravel and J. C. Woolley, Phys. Rev. B21 (1980) 659.
9) C. Hamaguchi, K. Miyatsuji and H. Hihara, Jpn. J. Appl. Phys. 23 (1984) L132.
10) K. Miyatsuji, H. Hihara and C. Hamaguchi, Superlattices and Microstructures, 1 (1985) 43.
11) H. Hihara and C. Hamaguchi, Solid State Communications, 54 (1985) 485.
12) P. J. Price, Ann. Phys. (N. Y.) 133 (1981) 217.
13) P. J. Price, J. Vac. Sci. Technol. 19 (1981) 599.
14) M. A. Littlejohn, J. R. Hauser and T. H. Glisson, J. Appl. Phys. 48 (1977) 4587.

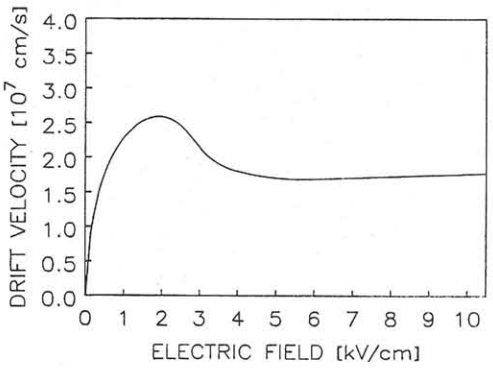

Fig. 1. Steady state drift velocity vs. electric field in SQW width 500A well and $N_s=1\times10^{12}$ cm^{-2} at 77K.

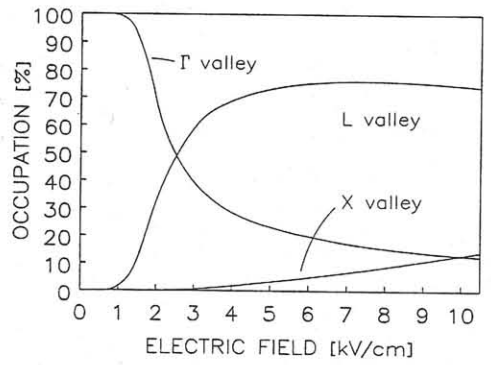

Fig. 2. Occupation of electrons vs. E in Γ-, L- and X-valleys at 77K.

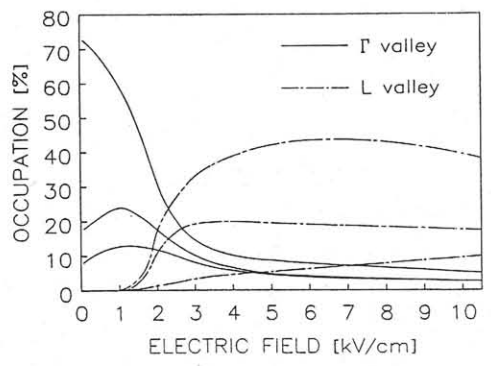

Fig. 3. Occupation of electrons vs. E in the three lowest subbands in Γ- and L-valleys at 77K.

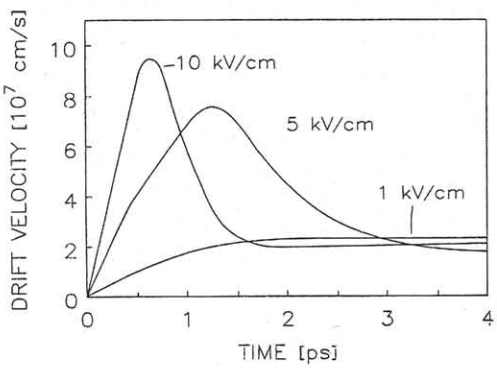

Fig. 4. Transient drift velocities in electric field of 1, 5 and 10 kV/cm at 77K.

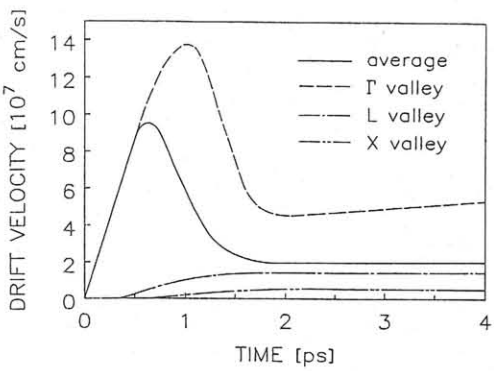

Fig. 5. Transient drift velocities in Γ-, L- and X-valleys at 10kV/cm and at 77K.

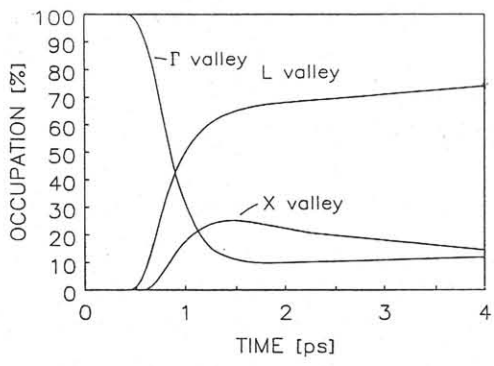

Fig. 6. Occupation of electrons vs. time in Γ-, L- and X-valleys at 10kV/cm and at 77K.